An Evaluation of ECMWF-Based Climatological Wind Stress Fields

ALBERTO M. MESTAS-NUÑEZ,* DUDLEY B. CHELTON, MICHAEL H. FREILICH, AND JAMES G. RICHMAN

College of Oceanic and Atmospheric Sciences, Oregon State University, Corvallis, Oregon

(Manuscript received 25 March 1993, in final form 21 October 1993)

ABSTRACT

A new mean monthly wind stress climatology based on seven years (1980–1986) of operational weather analyses by the European Centre for Medium-Range Weather Forecasts (ECMWF) has been derived by Trenberth et al. This climatology (referred to here as the TLO climatology) potentially represents a significant improvement over climatologies derived only from conventional wind observations. An attempt is made here to quantify the absolute accuracy of the TLO climatology by comparison with global wind stress fields constructed from vector winds measured by the Seasat-A Satellite Scatterometer (SASS) during 1978. From a simulated SASS dataset, it is shown that the magnitudes of the SASS stresses must be increased by about 7% to account for a systematic error that can be attributed to the scatterometer spatial- and temporal-sampling characteristics. After applying this correction, differences between the TLO climatology and SASS winds in the tropics are most likely related to known limitations of the ECMWF analyses. At latitudes south of 50°S, interannual variability and uncertainties in the operational weather analyses are so large that it is not possible to evaluate the TLO climatology on the basis of comparisons with SASS data. Outside of these equatorial and high southern latitude bands, the TLO stresses are shown to be systematically stronger than SASS by almost 50%. It is found that this difference can be entirely accounted for if the 1980–1986 ECMWF 1000-mb analyses are not interpreted as 10-m winds, as they were in constructing the TLO climatology. This conclusion is supported by an independent comparison of the synoptic ECMWF wind speed estimates with coincident buoy observations.

1. Introduction

A significant limitation to present-day modeling of ocean circulation is uncertainty in the wind stress over large areas of the global ocean. Large-scale ocean models have traditionally been forced with mean monthly climatic wind stress fields such as those derived from ship observations by Hellerman and Rosenstein (1983, hereafter HR). Because the vast majority of ship observations are confined to standard shipping routes, the quality of these wind stress fields in remote areas of the ocean is questionable.

A new mean monthly surface wind stress climatology has recently been computed by Trenberth et al. (1990, hereafter TLO; see also Trenberth et al. 1989), based on seven years (1980–1986) of twice-daily 1000-mb wind analyses from the European Centre for Medium-Range Weather Forecasts (ECMWF). The ECMWF analyses include significantly more ocean data than are available from ship reports alone, particularly over the Southern Hemisphere. In addition to the ship measurements, the analyses assimilate wind and sea level pressure observations from buoys and islands and atmospheric soundings of temperature, humidity, and velocity from radiosondes, upward-looking radars, and satellite observations. The first guess for the analysis at a particular time is given by past information that has been carried forward in time in a dynamically consistent way by numerical integration of the model. This first guess is updated at each analysis time to be consistent in a weighted least squares sense with the observations. The analyses have relatively coarse spatial (2.5°) and temporal (12 h) resolutions in addition to known inaccuracies in the tropics (Lambert 1988; Reynolds et al. 1989; Trenberth et al. 1989, 1990) and unknown accuracies in regions of sparse observations, particularly at high southern latitudes. An independent global estimate of the wind stress is needed to assess the accuracy of the TLO climatology, especially in the data-sparse regions.

In this study, high quality global estimates of near-surface winds over the ocean from satellite scatterometry are compared with the 7-year TLO wind stress climatology. The primary advantage of scatterometer data for evaluating the TLO climatology is that the spatial and temporal coverages are far better than those of any other observational system for surface vector winds. Three months of scatterometer data

* Current affiliation, Center for Air–Sea Technology, Mississippi State University, Stennis Space Center, Mississippi.

Corresponding author address: Dr. Dudley B. Chelton, College of Oceanic and Atmospheric Sciences, Oregon State University, Oceanography Admin. Bldg. 104, Corvallis, OR 97331-5503.

(7 July to 10 October 1978, only two months of which are used in this study—see section 2b) are available from the Seasat-A Satellite Scatterometer (SASS). Although of disappointingly short duration, these data have previously proven useful for identifying large, systematic errors in the HR wind stress climatology, particularly at high southern latitudes (Chelton et al. 1990). Other scatterometer data such as those from the Active Microwave Instrument (AMI) on board the European Space Agency ERS-1 satellite launched in July 1991 and the NASA scatterometer (NSCAT) to be launched in 1996 on board the Japanese ADEOS satellite promise wind observations over longer periods. These data products will be crucial for checking the quality of present wind climatologies and for developing a new, globally accurate climatology.

It is important to bear in mind that the differences between the SASS wind stress field and the 7-year TLO climatology are not necessarily indicative of errors in either dataset. The winds during the 1978 SASS observational period may not have been representative of the long-term mean and the differences from TLO must therefore be interpreted with caution. From the comparison of the SASS wind stress field with the HR climatology, Chelton et al. (1990) identified several regions of moderate interannual variability (up to 0.6 dyn cm^{-2} differences) north of 30°S. The differences between SASS and HR winds at higher southern latitudes were much larger (more than 2 dyn cm^{-2} in some regions). On the basis of Southern Hemisphere sea level pressure fields from the Australian Bureau of Meteorology (ABM), Chelton et al. (1990) argued that these differences at high southern latitudes are larger than can be accounted for by interannual variability alone; although July 1978 was highly anomalous, sea level pressure appeared to be nearly normal in the 3-month average July–September 1978.

Because the large-scale winds are approximately linearly related to the pressure fields, it can be inferred that the near-surface winds were approximately normal at high southern latitudes during this same period. However, surface wind stress is nonlinearly related to the vector wind field. Consequently, small deviations from the climatological average wind can be amplified in the stress fields. To use the SASS data for the assessment of the accuracy of the TLO climatology, a secondary objective of this study is therefore to attempt to determine how representative the wind stress field at high southern latitudes was of climatological conditions during the period sampled by SASS.

Another secondary objective of this study is to quantify the effects of sampling errors in spatially and temporally averaged wind stress fields constructed from SASS data. Although the quantity and geographical distribution of scatterometer data far exceed those of any other near-surface wind observations, the effects of the irregular and rather complex satellite sampling pattern on the accuracy of the wind fields is still a concern. This important issue has not been addressed by previous analyses of vector wind and wind stress fields constructed from scatterometer and simulated scatterometer data (e.g., Legler and O'Brien 1985; Chelton et al. 1989, 1990; Kelly and Caruso 1990).

Summaries of the data processing used to construct the TLO and SASS wind stress fields used in this study are given in section 2. The effects of sampling errors for the SASS instrument (including the actual gaps in the SASS dataset) are investigated in section 3. In section 4, the TLO wind stress climatology is shown to be systematically stronger than the SASS wind stress field at extratropical northern latitudes and middle southern latitudes. It is also shown that this systematic difference can be entirely eliminated when the ECMWF-based TLO wind stress climatology is recomputed with the ECMWF 1000-mb winds corrected to a height of 10 m by applying a multiplicative scaling factor derived on the basis of comparisons between the twice-daily ECMWF wind analyses and coincident buoy observations. The implication of these results is that the TLO wind stress climatology is sytematically high by almost 50%. A three-way comparison of the TLO climatology at high southern latitudes with wind stress fields constructed from SASS and ABM data in section 5 concludes that it is not possible to evaluate the quality of the TLO climatology south of 50°S.

2. Wind stress fields

a. ECMWF-based wind stress

The TLO mean monthly wind stress climatology was derived from 7-year vector averages (1980–1986) of twice-daily wind stresses computed from ECMWF 1000-mb winds on a $2.5° \times 2.5°$ grid. TLO argued that since ship wind observations were directly assimilated at the 1000-mb level prior to a model change in September 1986, the ECMWF 1000-mb winds for this period were more representative of the winds at a height of 10 m above the sea surface than at 1000 mb. The 1000-mb winds were therefore treated as 10-m winds in deriving the TLO climatology. In defense of this interpretation, Trenberth et al. (1989) cited Böttger (1982), who showed that the ECMWF 1000-mb winds compared favorably with surface observations at Ocean Weather Ship Lima (57°N, 20°W) for the first half of 1982, a period during which wind speeds were as high as 30 m s^{-1}. Some wave-modeling studies appear to offer additional support for the interpretation of the ECMWF 1000-mb analyses as 10-m winds; for example, Janssen et al. (1989) found that accurate wave predictions could be made when the ECMWF 1000-mb winds were treated as 10-m winds.

In the TLO climatology, the ECMWF assumed 10-m winds u_{10} were converted to surface wind stress using the bulk aerodynamic formula with the two-branch Large and Pond (1982) wind speed–dependent neutral-stability drag coefficient C_N extended to include two additional branches for wind speeds lower than 3 m s^{-1},

$$10^3 C_N = \begin{cases} 0.49 + 0.065u_{10}, & u_{10} > 10 \text{ m s}^{-1} \\ 1.14, & 3 \leq u_{10} \leq 10 \text{ m s}^{-1} \\ 0.62 + 1.56u_{10}^{-1}, & 1 \leq u_{10} \leq 3 \text{ m s}^{-1} \\ 2.18, & u_{10} \leq 1 \text{ m s}^{-1}. \end{cases} \quad (1)$$

The form of the 1–3 m s^{-1} wind speed branch was based on the notion that the drag coefficient increases as the wind speed approaches zero; the slope and intercept were calculated from the Large and Pond (1982) value of the drag coefficient at 3 m s^{-1} and empirical fits to the Dittmer (1977) and Schacher et al. (1981) drag coefficients at 2 m s^{-1} [see Fig. 2 of Trenberth et al. (1989)]. For wind speeds below 1 m s^{-1}, TLO fixed the neutral-stability drag coefficient at the extrapolated value pertaining to 1 m s^{-1}. The Large and Pond (1982) stability correction to the drag coefficient was applied directly to each gridded, synoptic ECMWF 1000-mb wind vector based on climatological mean monthly values of air and sea surface temperatures and relative humidity derived from the Comprehensive Ocean–Atmosphere Data Set (COADS). The air density needed to estimate wind stress by the bulk aerodynamic formula was computed individually for each ECMWF wind vector from the concurrent ECMWF estimates of air temperature, humidity, and pressure.

In section 4, the TLO wind stress climatology is recomputed after correcting for an apparent error in the TLO assumption that the ECMWF 1000-mb analyses were representative of 10-m winds. This corrected ECMWF-based climatology was generated using the TLO drag coefficient formulation (1). The Large and Pond (1982) stability correction to the drag coefficient requires both air and sea surface temperatures. The separate COADS air and sea surface temperature climatologies used by TLO were not readily available but their COADS climatological air–sea temperature difference field was. We used the Shea et al. (1990) mean monthly sea surface temperature climatology and derived a mean monthly air temperature field by combining the sea surface temperature climatology with the TLO air–sea temperature difference climatology. As in TLO, the air density used in the bulk aerodynamic formula to estimate wind stress was computed individually for each ECMWF wind vector from the concurrent ECMWF estimates of air temperature, humidity, and pressure.

b. SASS wind stress

The wind vectors used in this study were generated by Atlas et al. (1987), who removed the SASS directional ambiguities using an atmospheric general circulation model. This method gives good results for temporally and spatially averaged winds (Chelton et al. 1989). The SASS estimates of 19.5-m neutral-stability wind vectors were used to construct a 2-month vector average surface stress field by simple bin averaging on the ECMWF 2.5° × 2.5° grid for the period 1 August to 30 September 1978. The first month of SASS data was not included in this analysis because of evidence presented by Chelton et al. (1990) that the July 1978 wind field was anomalous south of 40°S.

The methodology used to construct the 2-month average wind stress field is essentially the same as that described by Chelton et al. (1990). Briefly, each SASS wind speed estimate was first corrected by subtracting a 1 m s^{-1} bias known to exist in the Atlas et al. (1987) SASS data. Because the SASS measurements of radar backscatter are calibrated to estimate neutral-stability winds at a height of 19.5 m, the appropriate scaling factor and drag coefficient to estimate surface wind stress are those corresponding to neutrally stable atmospheric conditions. The 19.5-m neutral-stability wind vectors were therefore reduced to winds at a height of 10 m by a multiplicative scaling factor of 0.943, computed from the boundary-layer model of Liu et al. (1979) for neutral stability. In the Southern Hemisphere, observations were eliminated south of a maximum ice boundary determined from passive microwave remote sensing (see Fig. 1 of Mestas-Nuñez et al. 1992).

Surface wind stress was computed for each SASS estimate of neutral-stability 10-m winds using the bulk aerodynamic formula with the TLO neutral-stability drag coefficient (1). Reliable global synoptic estimates of the air density needed in the bulk formulation were not available for the 1978 SASS observational period. It was therefore necessary to use a climatological mean monthly air density. This was computed on the 2.5° grid from the 7-year average of the twice-daily ECMWF estimates of air temperature, humidity, and pressure for the TLO period. Based on analysis of the seven years of the twice-daily ECMWF estimates of air density, the rms error introduced by using climatological air density rather than the actual air density in the bulk formula for wind stress is less than 1.5% globally.

As will be shown in the next section, contours of the 2.5° × 2.5° average wind stress from SASS exhibit a zonal quasi-periodic structure symptomatic of sampling errors in the 2-month average (see upper panel of Fig. 1). The bell-shaped low-pass filter described in detail in the appendix of Chelton et al. (1990) was applied to smooth the 2.5°-averaged

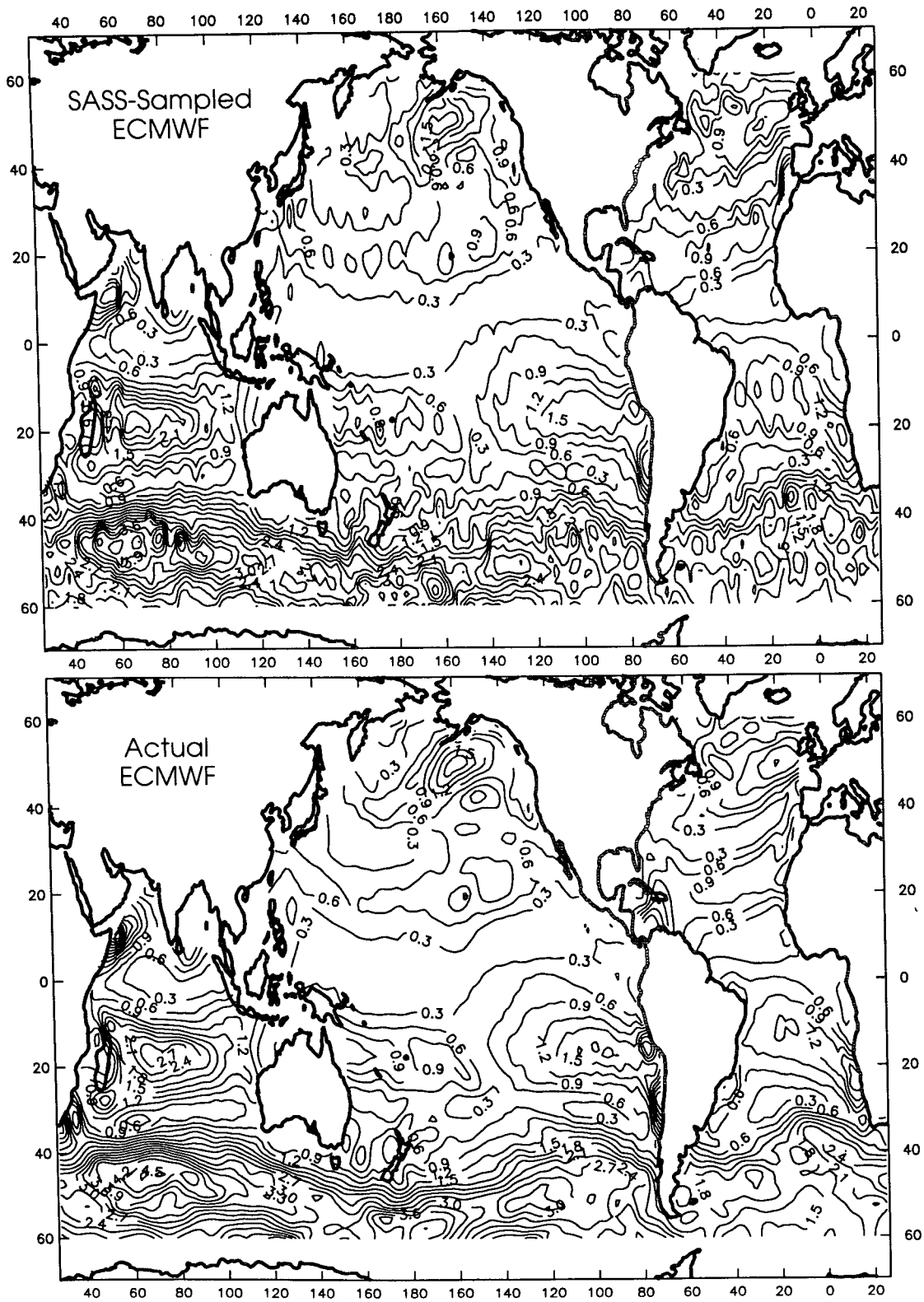

FIG. 1. Magnitude of the August–September 1985 vector-averaged wind stress constructed from the SASS-sampled ECMWF analyses (upper) and the complete ECMWF analyses (lower). Contour interval is 0.3 dyn cm^{-2}.

wind stress field with spatial resolution analogous to 5° latitude by 16° longitude moving averages, though with a sharper low-pass cutoff in the wavenumber domain. This smoothing also removes much of the short scale structure in the true wind field that is resolved by the SASS data but not by the ECMWF synoptic analyses, thus making the averaged SASS fields more compatible with the TLO climatology.

3. Scatterometer sampling error

As noted in the introduction, the spatial and temporal coverage of scatterometer data far exceed those of any other available wind observational system. For SASS and NSCAT, the wind field is sampled sequentially in time along the satellite orbit across two swaths of approximately 600 km width separated by a gap of about 400 km centered on the satellite ground track. The AMI on board the ERS-1 satellite samples the wind field over only one such swath and consequently has even greater problems with sampling errors than SASS or NSCAT. These spatial and temporal sampling characteristics are further complicated by spatial overlap of swaths from adjacent orbits at the higher latitudes and by overlap of measurements from ascending and descending orbits. The effects of this complex sampling pattern on the accuracy of spatially and temporally averaged wind stress fields constructed from scatterometer data have not previously been investigated.

An attempt to quantify the effects of SASS sampling errors is made here by simulating SASS measurements of a known wind field and directly comparing averages of the sampled values with the "true" mean quantities. The August–September 1985 twice-daily ECMWF surface analyses were used to define the "true" field, and the ECMWF 1000-mb winds were considered to be 10-m winds for the purposes of this analysis. Sample locations and times (relative to 0000 1 August) were taken from the actual SASS data. The SASS-sampled wind vectors were converted to wind stress using the method of TLO and then vector averaged over the 2-month period.

The ECMWF analyses define the "true" winds only at the model grid points in space and time. However, the SASS instrument had higher spatial resolution within the sample swaths and data were acquired continuously in time along the satellite orbit (rather than at the twice-daily analysis times). The simulation therefore requires interpolation of the ECMWF winds to the SASS measurement locations and times.

As noted by Schaefer and Doswell (1979), there is no unique method for interpolating a vector field. Even simple trilinear interpolation (in two spatial and one temporal dimension) is ambiguous, as systematically different results are obtained if the interpolation is carried out on components rather than on wind speed and direction. The direction of the interpolated wind vector can be obtained consistently by interpolating zonal and meridional components. However, the magnitude of the interpolated vector can be calculated either by interpolating scalar speeds or by taking the magnitude of the vector defined by the interpolated components. While the two results are identical when the direction of the wind field is spatially constant, the magnitudes obtained by interpolation of scalar speeds are systematically larger than the magnitudes from the component-wise interpolation when the wind direction changes across grid points [see Schaefer and Doswell (1979); the systematic difference is a simple manifestation of the Schwarz inequality]. Care must therefore be taken to assure that the results of the simulations are indicative of the effects of sampling errors, as opposed to interpolation errors.

The problem of the nonuniqueness of vector interpolation is addressed here by demonstrating that the results are not strongly dependent on the interpolation scheme used in the simulations. In the following, systematic errors in simulated SASS fields constructed by component-wise interpolation are compared with those in simulated fields constructed by scalar speed and direction interpolation.

Simulated SASS vector wind stress estimates were first obtained by linear space and time interpolation of each ECMWF vector wind component separately to the SASS sample times and locations. The magnitudes of the 2-month vector-averaged "true" and SASS-sampled wind stress fields for August–September 1985 are contoured in Fig. 1. The geographical patterns of high and low wind stress regions in the "true" field are clearly identifiable in the SASS-sampled field. However, the SASS-sampled field also exhibits a zonal wiggliness and patchiness of the contour lines. As the methodology used to compute the individual wind stresses and vector averages is exactly the same for both fields, this effect must be associated with sampling errors related to the SASS orbital characteristics. This is clear evidence that the similar structure noted in section 2b and seen previously by Chelton et al. (1990) in the gridded SASS wind stress fields indeed results from scatterometer sampling errors.

The upper panel of Fig. 2 shows that the Chelton et al. (1990) low-pass filter outlined in section 2b eliminates the sampling-related spatial structure of the SASS-sampled field. The same smoothing applied to the "true" 2-month average (lower panel of Fig. 2) results in only minor changes in the wind stress field; the contours are slightly smoother and the extrema of the high and low wind stress regions are reduced slightly in magnitude.

A scatterplot comparison between the smoothed "true" and the smoothed SASS-sampled fields (Fig. 3) shows that the scatterometer sampling introduces a systematic error in the wind stress magnitude. A least squares fit line through the origin of Fig. 3 (not shown)

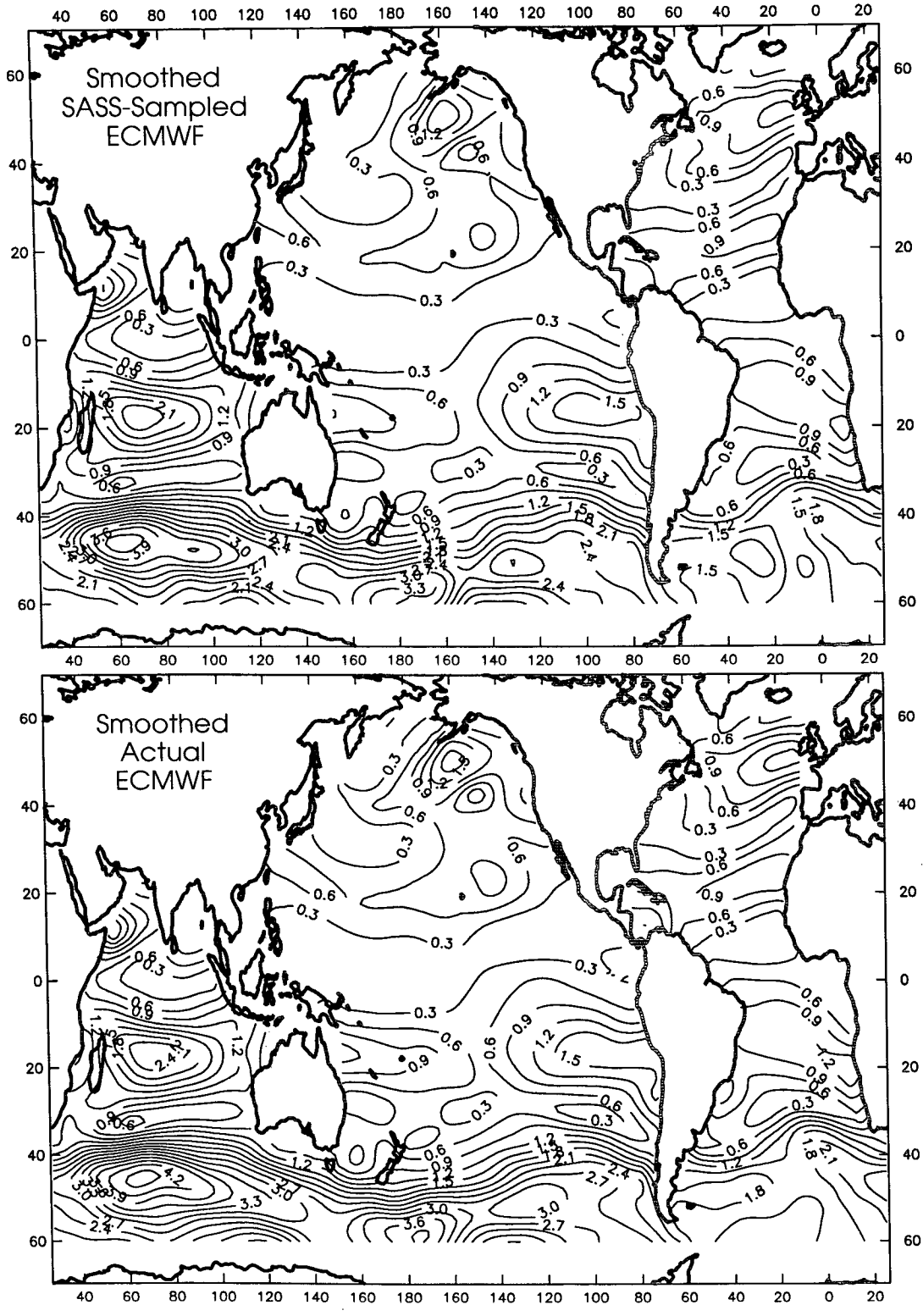

FIG. 2. Same as Fig. 1 except both fields have been smoothed as described in the text.

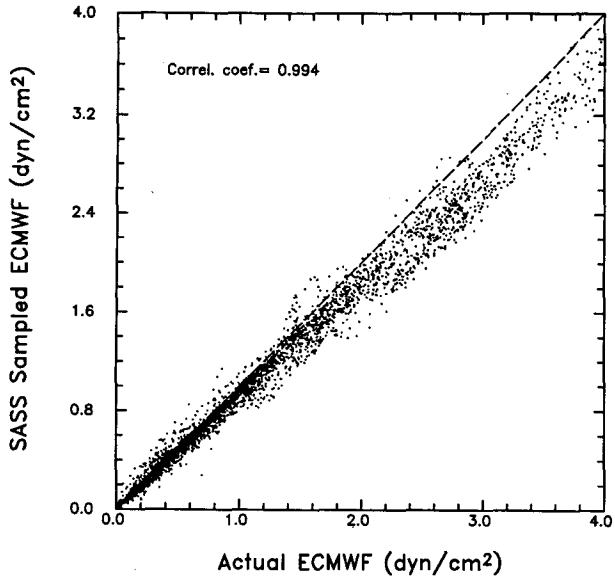

FIG. 3. Scatterplot comparison of SASS-sampled and ECMWF wind stress magnitudes for August–September 1985 in dynes per square centimeter.

has a slope of 0.90. The scatter in the comparison of the unsmoothed fields shown in Fig. 1 is larger but the slope is the same. On the basis of this comparison, the SASS sampling errors based on component-wise interpolation of the "true" winds thus result in a 10% underestimate of the magnitudes of 2-month vector average wind stresses.

When the SASS-sampled 2-month vector-averaged wind stress field is constructed from vector winds determined by the speed and direction interpolation technique, the regression coefficient increases to 0.97, which, as expected, is larger than the value obtained by the component-wise vector interpolation technique. Although the scaling factors differ somewhat, both vector interpolation methods indicate that the effects of SASS sampling errors are to reduce the magnitudes of the SASS-sampled 2-month vector-averaged wind stress field.

The conclusion that SASS sampling errors bias the 2-month vector-averaged wind stress fields low was further investigated by a third analysis consisting of comparisons between "true" and SASS-sampled 2-month scalar-averaged wind stress magnitudes. After linearly interpolating the wind speeds to the SASS observation times and locations, computing the wind stress magnitude corresponding to each interpolated wind speed and then scalar averaging over the 2-month period, the regression coefficient for the comparison was found to be 0.93. This 7% underestimate of the scalar wind stress magnitude field computed from the simulated SASS data lies halfway between the 0.97 and 0.90 values deduced from vector averaging using the two vector interpolation methods.

All three methods of comparing the "true" and SASS-sampled wind stress fields thus lead to a consistent conclusion that sampling errors result in a systematic underestimate in the 2-month average wind stress fields derived from SASS observations. That the 2-month vector-averaged wind stress estimates are systematically low in the SASS-sampled data is not surprising. Wentz et al. (1986) have pointed out that wind speeds are approximately Rayleigh distributed. Because of the irregular temporal sampling interval of scatterometer data and the asymmetry of the Rayleigh distribution, the probability of observing high wind speed events within a given 2.5° region is lower than that of observing low wind speed events, thus biasing the magnitudes of averaged wind fields low.

From the above estimates of sampling errors, we recommend increasing the magnitude of wind stress estimates obtained from SASS wind observations by 7% when using the bulk formula with 2-month vector averages. Such a correction is equivalent to increasing the drag coefficient by 7% to compensate for scatterometer sampling errors when computing stress from SASS wind vectors. Hereafter, SASS wind stress fields inflated by 7% are referred to as "corrected SASS" fields.

4. TLO and SASS wind stress comparison

Meridional profiles of the zonally averaged eastward components of TLO and corrected 2-month vector-averaged SASS wind stress estimates are shown in Fig. 4. The shaded region represents the ±2 standard deviation range of interannual variability over the seven individual August–September vector-averaged ECMWF wind stress fields for the 1980–1986 period from which the TLO climatology is constructed. Interannual variability is largest in the major wind belts, particularly in the Southern Hemisphere westerlies. In general, the profile derived from SASS data falls within the range of natural variability, complicating the ability to distinguish systematic errors in the wind stress estimates from differences associated with interannual variability. In the tropics, however, the difference between SASS and TLO wind stress profiles exceeds the 2 standard deviation range of interannual variability, suggesting an error in one or both of the fields.

After removal of the 1 m s^{-1} bias as discussed in section 2b, there is no documented evidence for any geographical dependence of the accuracies of SASS winds that would account for errors in the SASS wind stress magnitudes in the tropics (Davison and Harrison 1990). In contrast, Lambert (1988), Reynolds et al. (1989), Trenberth et al. (1989), and TLO have all noted shortcomings of the ECMWF analyses in the tropics, apparently arising from limitations in the ability of the model to analyze the divergent component of the vector wind field in the highly convective tropical

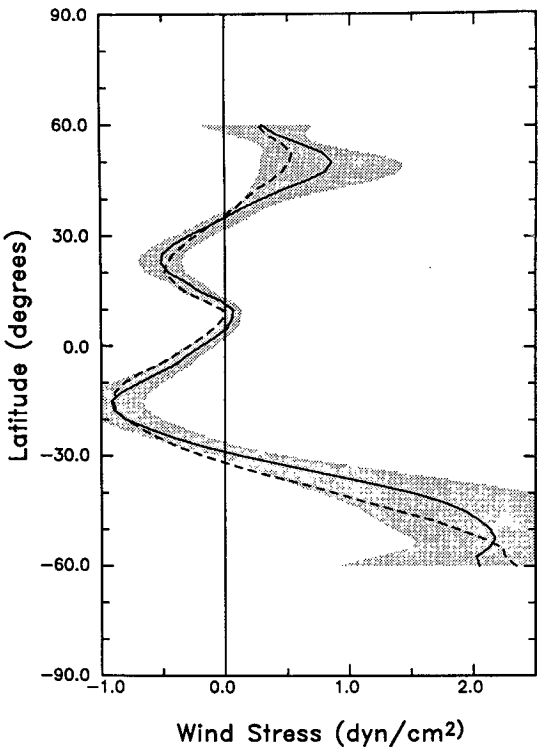

FIG. 4. Latitudinal profiles of zonally averaged eastward components of wind stress from the August–September TLO climatology (solid line) and corrected SASS (dashed line) in dynes per square centimeter. The ±2 standard deviation range of natural variability of ECMWF-based wind stress fields during the seven years from which the TLO climatology was constructed is indicated by the shading.

regions. The differences between the SASS and TLO wind stress fields in the tropics therefore most likely arise from errors in the ECMWF analyses. The TLO climatological wind stress estimates within the tropical regions (conservatively defined here to be within ±25° of the equator) are therefore not considered further in this study.

The August–September TLO and corrected SASS average and difference wind stress fields generated as described in section 2 are shown in Fig. 5. For consistency, the TLO wind stress field has been smoothed in the same manner as the SASS wind stress field as described in sections 2b and 3. At middle latitudes in the Pacific and Atlantic oceans, the two wind stress fields generally agree to within 0.3 dyn cm^{-2}. Previous comparisons of SASS with HR (Chelton et al. 1990) suggested that most of the differences in the Northern Hemisphere could be attributed to apparent anomalous wind stress during the SASS sampling period. The same conclusion can be drawn here from the SASS and TLO comparison. For example, the band of large differences along 45°N in the North Atlantic is apparently an indication that the westerlies were weaker than normal during the Seasat mission since a similar feature is present in the September differences between SASS and HR. Similarly, the small regions of significant differences off the northwest U.S. coast, the Somali coast, and in the western tropical Pacific are also present in the SASS minus HR wind stress fields.

Some other Northern Hemisphere differences in Fig. 5 may be attributable to anomalous winds during the TLO sampling period. For example, the region of 0.6 dyn cm^{-2} differences south of the Aleutian Peninsula is not present in the differences between SASS and HR (see Fig. 10 of Chelton et al. 1990). This feature is probably related to the deeper-than-normal Aleutian low during the 1980–1986 period noted by TLO.

The main feature of the SASS and TLO difference field in Fig. 5 is the band of very large differences at high southern latitudes where the generally eastward TLO wind stress is much stronger than the SASS wind stress. The maximum difference exceeds 1.8 dyn cm^{-2} in the Indian Ocean sector of the Southern Ocean. From Fig. 4, interannual variability in the ECMWF analyses is largest at high southern latitudes. Evaluation of the TLO climatology is therefore more problematic in this region than elsewhere; discussion of the wind stress field south of 50°S is therefore deferred to section 5.

Stress-dependent systematic differences between the SASS and TLO wind stress fields at extratropical northern and middle southern latitudes can be identified even in the presence of the "noise" introduced by interannual variability. The differences between the magnitudes of the two vector-averaged wind stress fields were binned into 0.1 dyn cm^{-2} intervals according to the average of the two wind stress magnitudes. As described previously by Wentz et al. (1986) and Chelton and Wentz (1986), this method of presentation is preferable to the more traditional scatterplot comparison between the the SASS and TLO wind stress magnitudes because it avoids introducing artificial biases at high and low winds; at a location where one of the wind stress estimates is extreme (high or low), it is likely that the other will be less extreme.

The mean and ±1 standard deviation of the TLO minus SASS wind stress magnitude differences are displayed as a function of the mean stress in Fig. 6 for three latitudinal bands. It is apparent that the scatter within each 0.1 dyn cm^{-2} bin from interannual variability averages to near zero. This averaging isolates a systematic difference between the two wind stress fields. In the extratropical northern and middle southern latitude bands, the differences between the TLO and SASS wind stress fields are very similar and suggestive of a simple scaling difference. From a least squares fit line through the mean differences, the TLO wind stresses are systematically stronger than SASS by 45.7% in the extratropical northern latitudes (25°N to 60°N) and by 46.4% in the middle southern latitudes (25°S to 50°S).

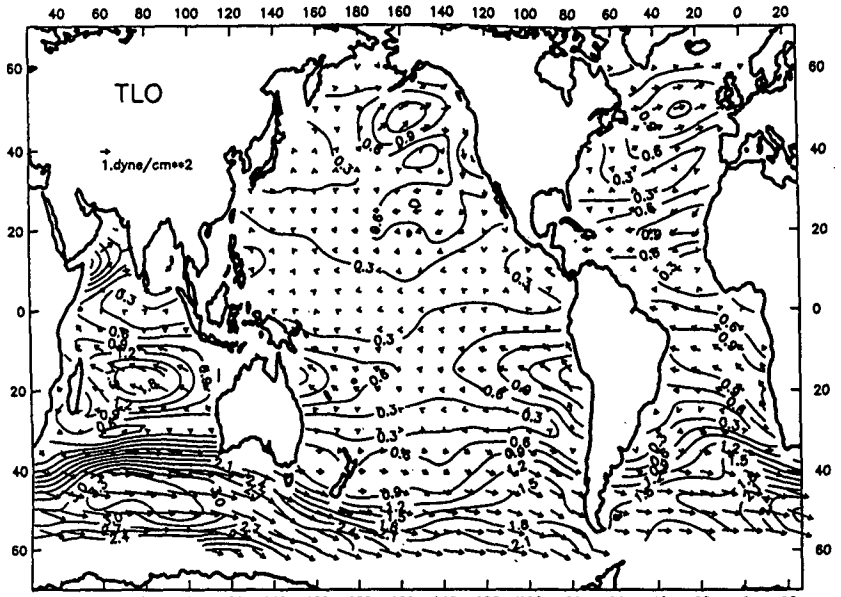
TLO
1.dyne/cm**2

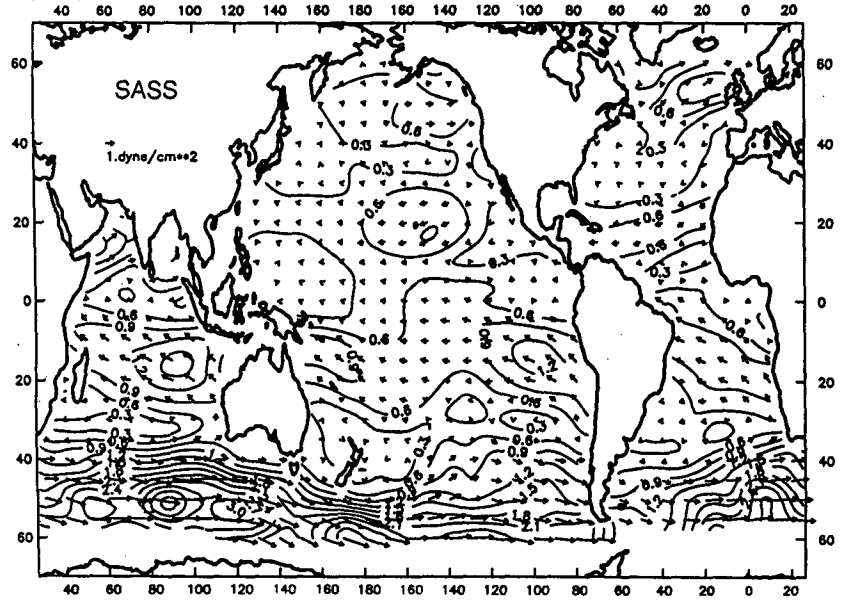
SASS
1.dyne/cm**2

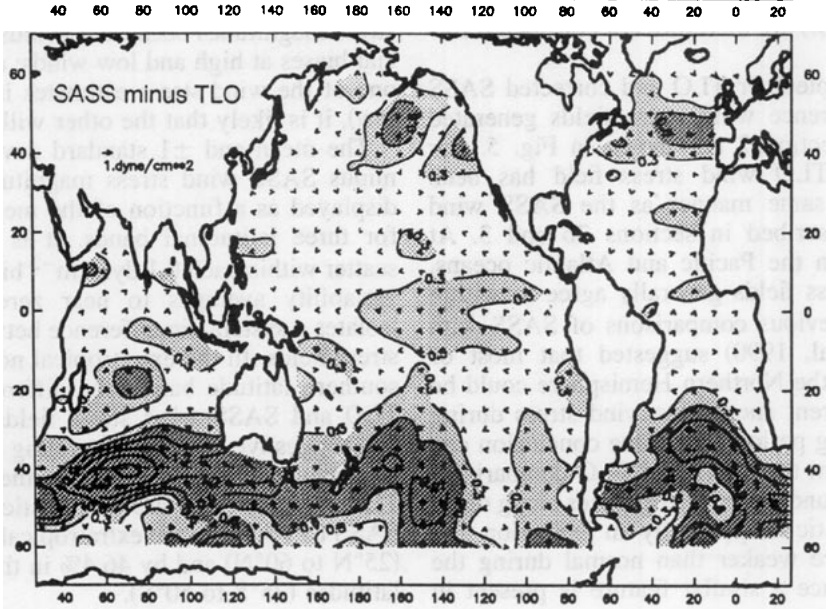
SASS minus TLO
1.dyne/cm**2

The large and consistent differences between the binned TLO and SASS wind stress magnitudes in Figs. 6a and 6b are almost certainly indicative of systematic errors in one of the fields rather than global-scale interannual variations in the wind stress field. After unsuccessfully exploring several other candidate explanations for these differences, we eventually investigated the possibility that the TLO interpretation of ECMWF 1000-mb winds as 10-m winds might be incorrect. To test this hypothesis, some other reliable independent estimate of the winds is required. Moored buoy data from the National Data Buoy Center (NDBC) (Meindl and Hamilton 1992) are well suited to such purposes. The NDBC anemometer heights ranged from 5 to 20 m, with an average of 8.6 m. The NDBC dataset includes the air and sea surface temperature measurements required for boundary-layer conversions of the buoy winds to a consistent reference height of 10 m. These buoys are located in the Northern Hemisphere primarily along the U.S. coasts. Only the open-ocean buoys north of 25°N were considered for this study to avoid problems in the interpretation of the gridded ECMWF analyses near continental boundaries and in the tropical latitudes. All of the NDBC buoys analyzed here were more than 100 km from land and most of them were more than 200 km from land. The locations of the open-ocean NDBC buoys for August 1980 and September 1985, as well as the nearest ECMWF grid points, are shown in Fig. 7. The buoy distributions during these two months are representative of the 7-year period 1980–1986 from which the TLO climatology was constructed.

The NDBC hourly 8-min averages of wind speed were adjusted to a reference height of 10 m, taking into account the stability of the atmosphere (Large and Pond 1982). Although some selected recent NDBC buoys measure relative humidity, this was not the case with the buoys considered during the period of interest in this study. Atmospheric stability was therefore estimated from the buoy measurements of air–sea temperature difference and the climatological mean monthly relative humidity derived from COADS data by TLO (see section 2a). The buoy estimates of 10-m wind speeds for the August–September periods of 1980–1986 were then compared with concurrent twice-daily ECMWF 1000-mb wind speeds at the nearest ECMWF grid locations.

The results are shown in Fig. 8, which has the same format as Fig. 6; the mean differences between the two estimates of wind speed are plotted against their average in 0.4 m s^{-1} bins. A least squares analysis of this comparison of 7378 buoy and ECMWF wind speeds indicates that the ECMWF speeds are 16.5% too high. The corresponding scaling factor of $1/1.165 \approx 0.86$ necessary to reduce the ECMWF 1000-mb wind speeds to the values consistent with coincident 10-m buoy wind speeds falls within the 0.7–0.9 range of published reduction coefficients for converting model isobaric and geostrophic winds to surface winds (e.g., Findlater et al. 1966; Aagaard 1969; Hasse and Wagner 1971; Clarke and Hess 1975; Willebrand 1978; Reynolds et al. 1989; Lalbeharry et al. 1990; Chelton et al. 1990; Freilich and Dunbar 1993). The systematic difference between ECMWF 1000-mb winds and 10-m NDBC buoy winds in Fig. 8 thus suggests that the ECMWF 1000-mb analyses during the 1980–1986 period really are representative of 1000-mb winds rather than of 10-m winds as assumed by TLO.

When the vector-averaged TLO climatology is recomputed as described at the end of section 2a after reducing the ECMWF wind speeds by 14% to convert the 1000-mb winds to 10-m winds, the systematic differences between the 2-month vector average SASS and TLO wind stress estimates are completely eliminated (Fig. 9). Thus, as a consequence of the apparent scaling error, the wind speed dependence of the drag coefficient and the two-month vector averaging, the magnitudes of the wind stresses in the TLO climatology are too high by almost 50%. We conclude that the ECMWF 1000-mb winds during the 1980–1986 period should not be interpreted as 10-m winds.

This conclusion may have significant implications for the wave-modeling results that evidently formed part of the basis for treating the ECMWF 1000-mb analyses as 10-m winds in the TLO climatology. Wave predictions are very sensitive to errors in the wind stress fields used to force the wave model (Janssen et al. 1989; Beal 1991; Lionello et al. 1992), with 10% errors in wind speeds resulting in approximately 20% errors in wave height predictions. Operational wave models are forced by twice-daily wind stress fields derived from operational analyses like the ECMWF analyses used to construct the TLO climatology. A proper interpretation of the weather model "surface winds" is clearly important when calculating the stresses used to force the wave models.

The exact procedures used by wave modelers when calculating surface stresses from operational weather analyses are often vague. Furthermore, errors in the wave models themselves can be compensated for by errors in the wind stress forcing. For example, in the recent study by Lionello et al. (1992), an

FIG. 5. August–September vector-averaged wind stress from the TLO climatology (upper) and from corrected SASS (middle). Both wind stress fields have been smoothed as described in the text and the contour interval is 0.3 dyn cm^{-2}. The wind stress differences (SASS minus TLO) are shown in the lower panel, with differences larger than 0.3 dyn cm^{-2} lightly shaded and differences larger than 0.6 dyn cm^{-2} heavily shaded.

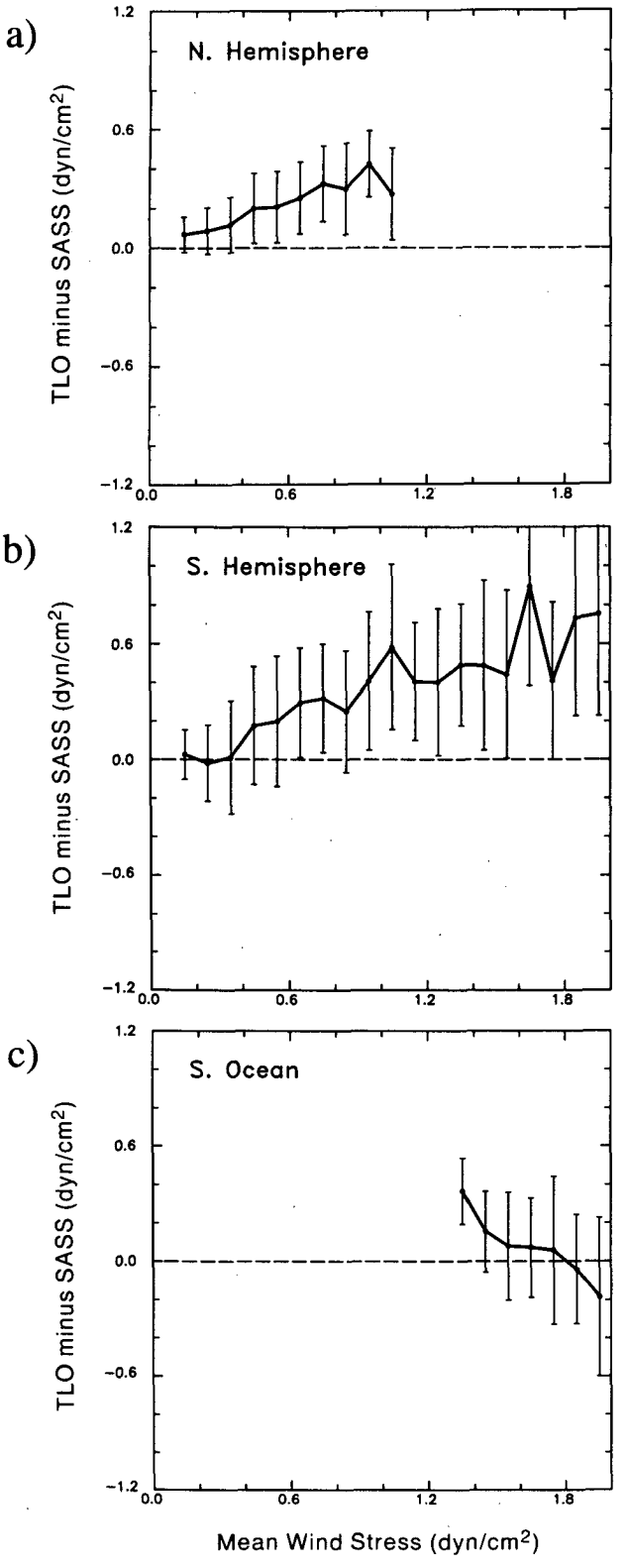

FIG. 6. Comparisons betweeen the magnitudes of the TLO and corrected SASS vector-averaged wind stress fields (a) in the extratropical Northern Hemisphere between 25°N and 60°N; (b) in the midlatitude Southern Hemisphere between 25°S and 50°S; and (c) in the Southern Ocean south of 50°. The mean differences (TLO minus SASS) and ±1 standard deviations are plotted against the average of the two wind stress estimates in 0.1 dyn cm^{-2} bins.

operational wave model forced by ECMWF-based wind stress fields was shown to overpredict wave heights within storm regions, but to overestimate the dissipation, and hence underpredict wave heights, outside of the immediate area of the storm system. The model therefore underpredicted wave heights in a global average sense. Increasing the magnitude of the wind stress forcing (by, for example, substituting 1000-mb winds for the 10-m winds used to force the model) could thus apparently offset errors in the wave model, increasing the overall skill of the wave model. Compensating errors such as these may in fact be responsible for the unreferenced TLO statement that treating the ECMWF 1000-mb winds as 10-m winds yielded more accurate wave model predictions.

5. The high southern latitude wind stress field

The qualitative impact of the apparent overestimate of wind stress in the TLO mean monthly climatology on ocean modeling can be investigated using the Sverdrup model. In this simple linear model, a 46% overestimate of wind stress results in a 46% overestimate of transport everywhere, but leaves the patterns of circulation unchanged. The effects of such large errors in the wind stress on more sophisticated ocean circulation models may differ in magnitude and are likely to be much more complex spatially but are almost certainly significant.

The Sverdrup circulations derived from the corrected SASS wind stress field and from the corrected TLO wind stress field are shown in Fig. 10. The large differences between the two estimates of Sverdrup circulation in the tropical Pacific further emphasize the weaknesses known to exist in the ECMWF analyses in this region. The most striking feature in Fig. 10 is the exceptionally large differences between the two estimates of Sverdrup circulation at high southern latitudes; streamfunction differences larger than 50 Sv (1 Sv $\equiv 10^6$ m^3 s^{-1}) are found in the Indian and Atlantic sectors of the Southern Ocean. The line of zero wind stress curl in the SASS data is displaced considerably more southward (about 5° in the Indian Ocean and more than 10° in the Atlantic) than in the TLO data (Fig. 11). This may be indicative of anomalous atmospheric conditions during the 1978 SASS observational period (Trenberth and van Loon 1981; Trenberth 1984). Alternatively, the possibility of systematic errors in the ECMWF analyses at these latitudes cannot be discounted. The large differences between the two circulations underscore the importance of determining the accuracies of presently available climatological wind stress fields for ocean circulation modeling at high southern latitudes.

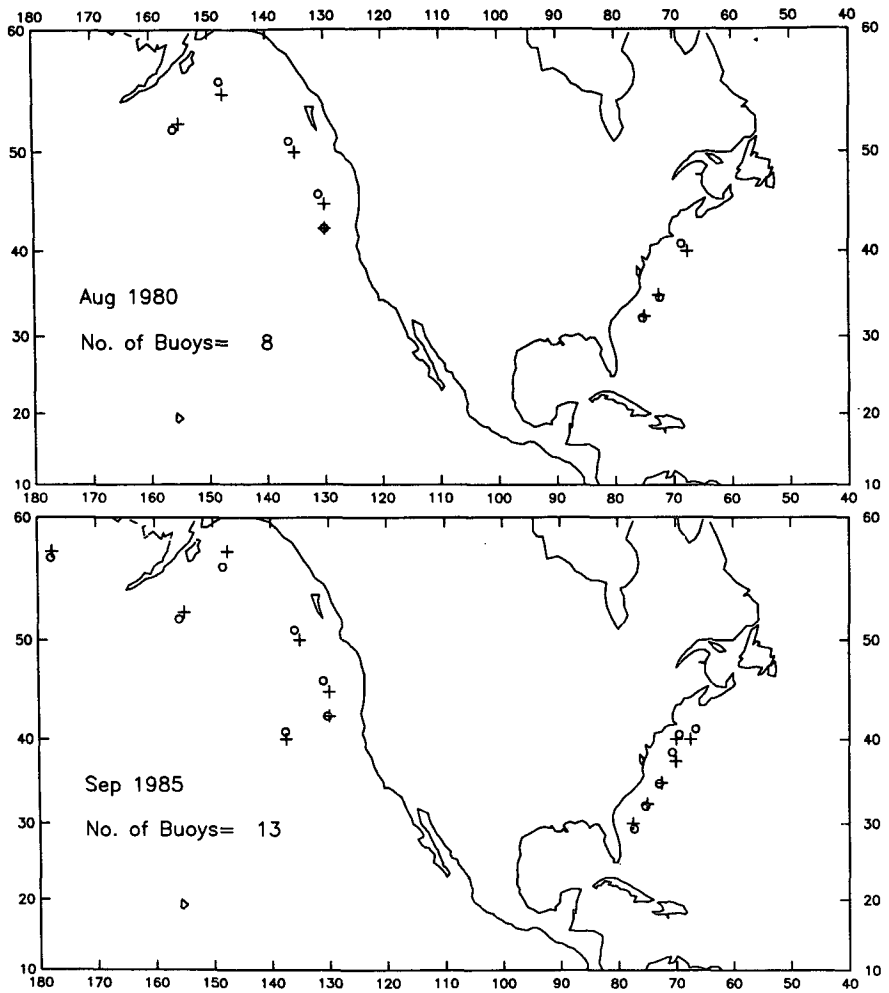

FIG. 7. Maps of the National Data Buoy Center (NDBC) buoy locations (open circles) for August 1980 (upper) and September 1985 (lower). The locations of the nearest ECMWF grid points are indicated as plus symbols.

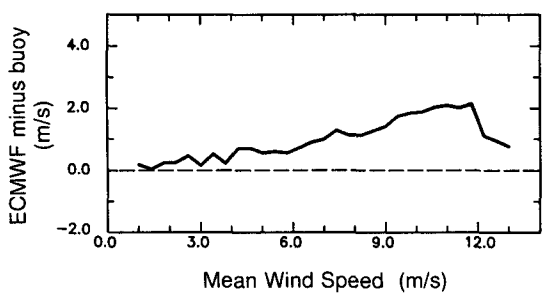

FIG. 8. Comparisons of 7378 concurrent synoptic ECMWF and NDBC buoy wind speeds for the August–September periods of 1980–1986. The mean differences (ECMWF minus buoy) are plotted against the average of the two estimates in 0.4 m s^{-1} bins.

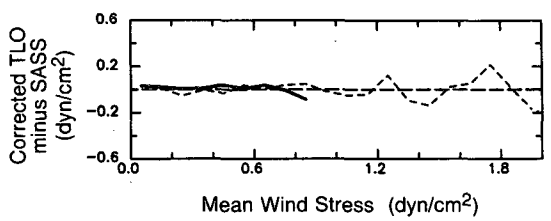

FIG. 9. Comparisons of corrected SASS and corrected TLO wind stress fields for August–September in the extratropical Northern Hemisphere (solid line) and the midlatitude Southern Hemisphere (dashed line).

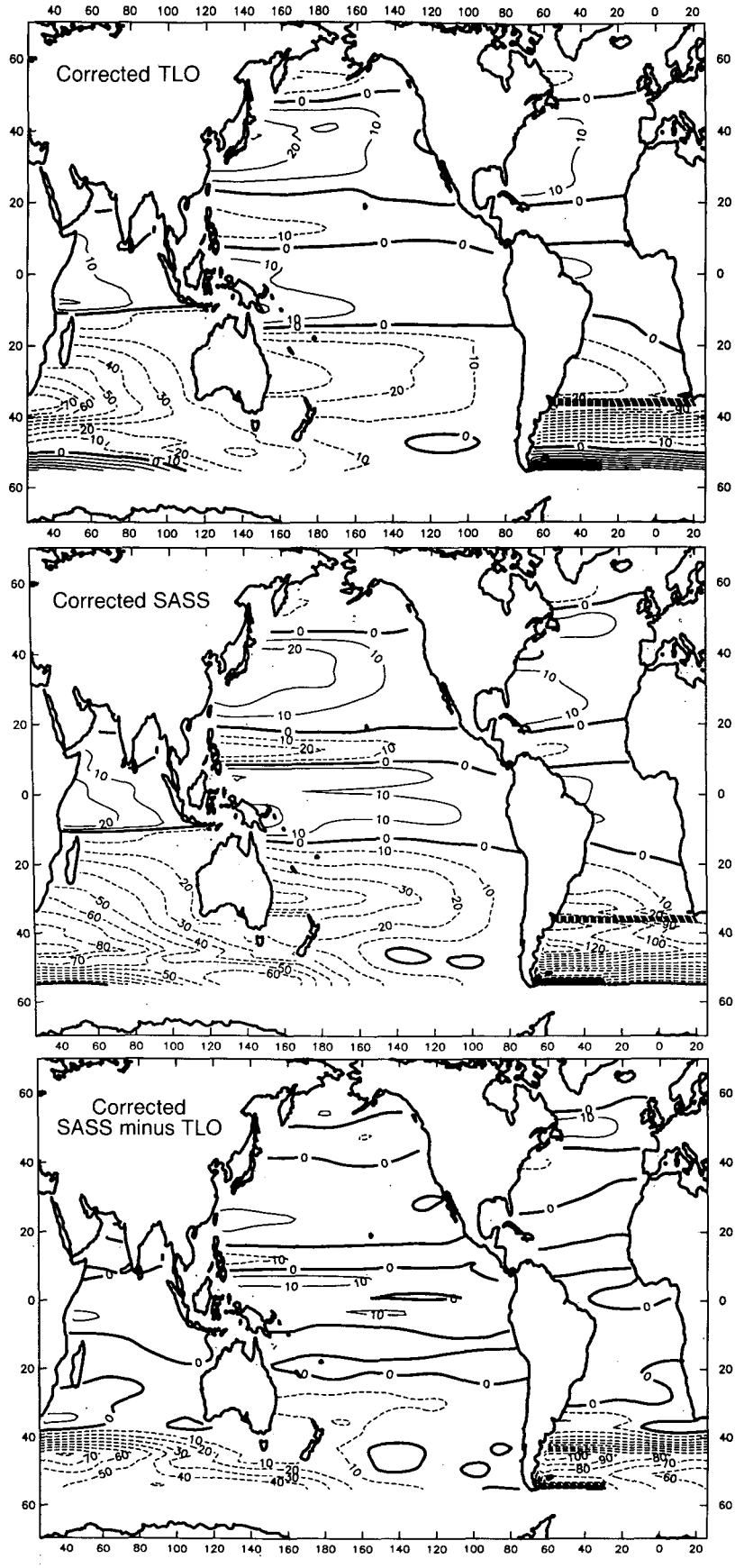
Corrected TLO
Corrected SASS
Corrected
SASS minus TLO

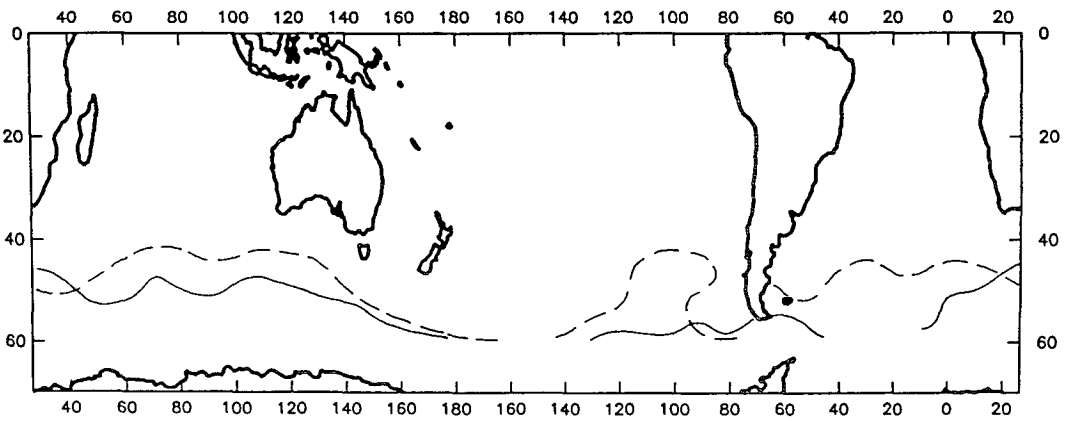

FIG. 11. The line of zero wind stress curl in the Southern Hemisphere westerlies from the August–September 1978 SASS data (solid line) and the August–September 1980–1986 TLO climatology (dashed line).

Assessing whether the high southern latitude wind stress field was climatologically normal during the SASS 1978 observational period is very difficult. In the Southern Ocean latitude band, where interannual variability is large, as discussed previously, the mean differences between the gridded SASS wind stress values and the TLO climatology are smaller in all but one of the bins than the standard deviation of interannual variability (Fig. 6c). It is generally agreed that the ECMWF analyses are presently the most accurate operational weather analyses available globally. However, it is also generally conceded that the best available Southern Hemisphere weather analyses during 1978 were those produced by the Australian Bureau of Meteorology (ABM) [e.g., see Figs. 9 and 10 of Trenberth and Christy (1985)].

We compared the ABM and ECMWF analyses by computing an independent mean monthly vector-averaged wind stress climatology from the ABM analyses of 1000-mb winds for the 1980–1986 period (the same period used to construct the TLO climatology). From empirical analysis, we found that a very close agreement between the ABM and corrected TLO wind stress fields could be obtained when each gridded ABM 1000-mb vector wind is reduced in magnitude by 21% and rotated 14° counterclockwise prior to computing the vector-averaged wind stress.

The differences between the two 7-year wind stress climatologies are shown in Fig. 12a. Over most of the Southern Hemisphere, the differences are very small. The most significant difference is the 0.3 dyn cm^{-2} dipole south of Australia that arises because the jet stream in this region is apparently displaced to higher southern latitudes in the corrected TLO climatology than in the ABM climatology. The 21% scaling factor can be compared with the 14% scaling factor deduced in section 4 for converting the ECMWF 1000-mb analyses to 10-m winds. As noted above, both scaling factors are within the range of values used in previous studies to convert model isobaric and geostrophic winds to surface winds. The somewhat larger scaling factor and the 14° rotation angle required to optimize the agreement between the ABM and TLO climatologies apparently indicate that the ABM analyses are representative of somewhat higher altitude winds than the Southern Hemisphere ECMWF analyses. For present purposes, the important point is that the wind stress fields produced from the two operational weather analysis models are remarkably consistent for the 1980–1986 period after appropriate scaling adjustments.

Although there is no assurance that the ABM analyses during 1978 were of comparable quality to the 1980–1986 ABM analyses, an attempt can be made to determine how anomalous the wind stress field was during the Seasat period by comparing the August–September 1978 ABM wind stress field with the 1980–1986 ABM climatology for the August–September period. The difference field (Fig. 12b) suggests that, in 1978, the maximum surface stress associated with the Southern Hemisphere westerlies was displaced southward between about 80°E and 180°. However, a comparison between the August–September 1978 ABM wind stress field and the concurrent SASS wind stress field (Fig. 12c) casts doubt on the quality of stress fields derived from the ABM

FIG. 10. Sverdrup transport streamfunction field constructed from the corrected August–September TLO wind stress field (top) and the corrected SASS wind stress field (middle). The difference field (SASS minus TLO) is shown in the lower panel. Contour interval is 10 Sv (1 Sv $\equiv 10^6$ m^3 s^{-1}). The computational details of these Sverdrup circulation fields are described by Chelton et al. (1990) and Mestas-Nuñez et al. (1992).

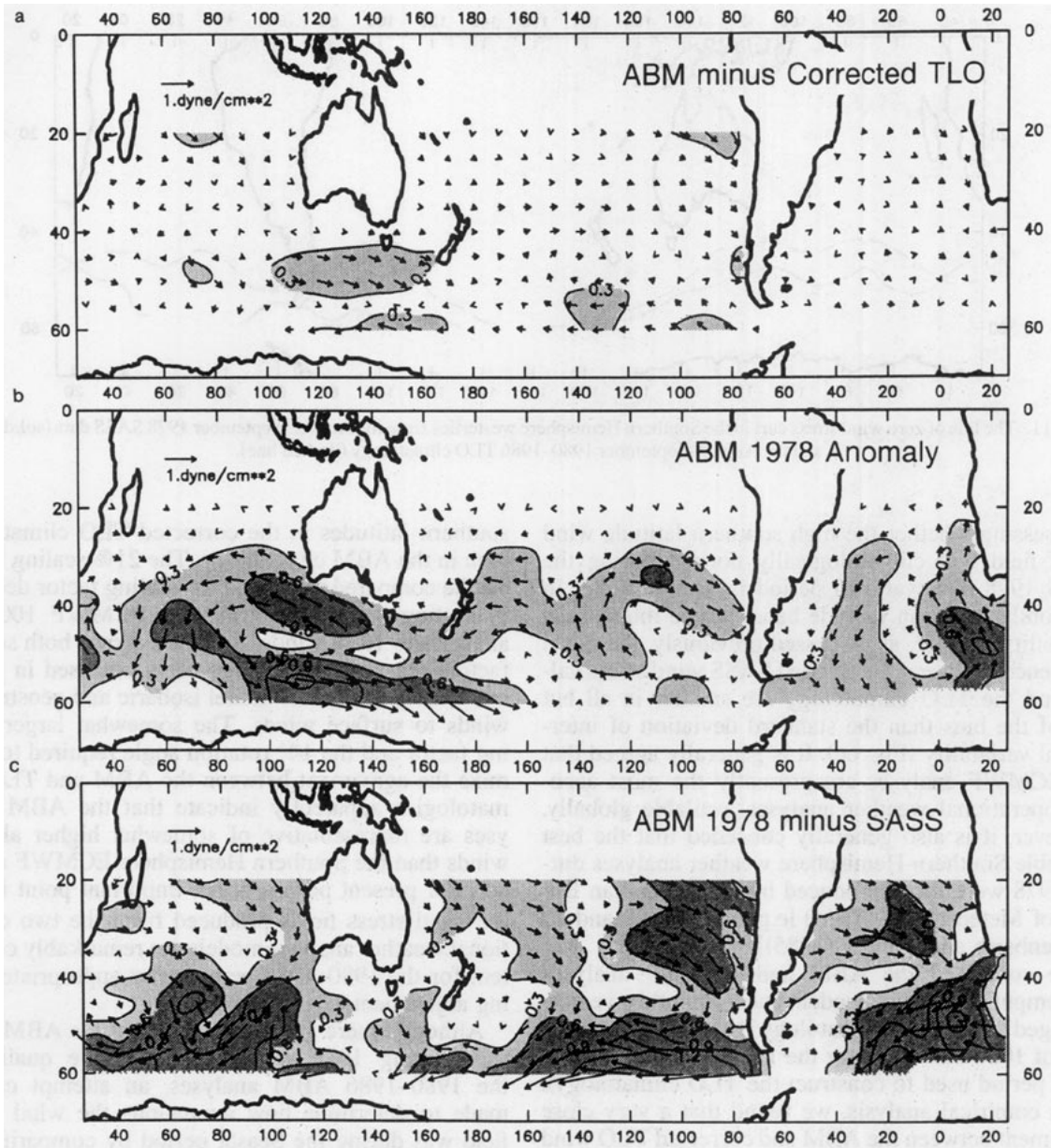

FIG. 12. Differences between (a) the ABM and TLO 7-year average August–September wind stress fields (both corrected as described in the text); (b) the August–September 1978 ABM wind stress and the 7-year ABM climatological average for the same period; and (c) the August–September 1978 ABM wind stress and the corrected SASS wind stress for the concurrent period.

analyses during this period; there is very little correspondence between Figs. 12b and 12c. Differences of more than 0.6 dyn cm^{-2} between the ABM and SASS wind stresses are common at latitudes higher than 50°S. While the possibility that SASS winds are less accurate at high southern latitudes than at other latitudes cannot be totally discounted, this seems highly unlikely from all the analyses of SASS data carried out to date. On the other hand, it is easy to imagine limitations in the accuracies of operational analyses (contemporary as well as during 1978) in this region of sparse observational data.

The analysis in this section unfortunately sheds little definitive light on the accuracy of climatological wind stress fields at high southern latitudes. The consistency between the corrected TLO and ABM wind stress fields for the 7-year period 1980–1986 is encouraging. However, the large discrepancies between SASS and ABM wind stress fields during August–September 1978 are highly suggestive of errors in the

ABM analyses during this time period. This implies that the quality of the TLO and ABM wind climatologies at high southern latitudes must be considered suspect; unless there were major improvements in the quality of the ABM analyses between 1978 and the 1980–1986 period, the more recent ABM, as well as the ECMWF, analyses also likely contain large systematic errors. This could account for the large discrepancies in Fig. 5 between the SASS and TLO wind stress fields at high southern latitudes. We conclude that a longer record of scatterometer measurements will be necessary to produce a reliable wind stress climatology at high southern latitudes.

One feature of the Sverdrup circulations shown in Fig. 10 that merits some discussion is the westward transport south of Australia and New Zealand. This westward transport is weaker in the Sverdrup circulation calculated from the TLO wind stress than in that calculated from the SASS wind stress, but is nonetheless unambiguously present. The existence of westward Sverdrup transport in this region has previously been discussed by Godfrey (1989) and Chelton et al. (1990), who have also noted that the sparse historical hydrographic data in this region support the possibility of westward transport.

Although westward transport in this region is highly inconsistent with the conventional view of the Antarctic Circumpolar Current (ACC) as a strong eastward flow throughout the Southern Ocean, there is mounting evidence for a strong tendency for westward wind-driven transport from all available wind stress fields (HR, TLO, ABM, and SASS), despite limitations in each of the various wind stress fields. The existence of westward transport equatorward of the ACC is further supported from recent hydrographic measurements (J. Church 1993, personal communication) and 1000-m float trajectories (R. Davis 1993, personal communication). The core of the ACC with eastward velocity of about 50 cm s^{-1} is centered at about 50°S south of Australia, but westward velocities of 10–20 cm s^{-1} are found as far south as about 48°S.

6. Summary and discussion

In this study, Seasat scatterometer (SASS) observations and NDBC buoy observations of winds have been used to investigate the accuracy of the Trenberth et al. (1990) ECMWF-based mean monthly wind stress climatology. Although the August–September 1978 scatterometer data are not contemporary with the 1980–1986 TLO climatology, they do offer the advantage of providing a global dataset for comparison. The extent to which such a comparison is useful depends upon the degree to which systematic errors can be detected in the presence of interannual variability. The consistency between the SASS-ECMWF comparisons in Fig. 6 and the independent point comparisons of ECMWF winds with contemporaneous buoy observations in Fig. 8 support an interpretation that the effects of interannual variability are largely eliminated in the binned average scatterplots in Fig. 6 for the Northern Hemisphere and middle latitudes of the Southern Hemisphere; the scatter within each 0.1 dyn cm^{-2} bin from interannual variability averages to near zero.

An important problem with the SASS data is the error introduced by irregular sampling in space and time. The analysis of section 3 demonstrates that the overall effects of SASS sampling can be diminished by inflating the magnitude of the mean SASS wind stress vectors by about 7%. This result has important implications for the Chelton et al. (1990) comparison of 3-month vector-averaged SASS and HR wind stress fields. Although the systematic underestimate of time-averaged wind stress fields arising from SASS sampling characteristics should have been obvious in that study, as well as in other scatterometer studies (e.g., Legler and O'Brien 1985; Kelly and Caruso 1990), it has been overlooked until now. One reason for this oversight is that the 19% difference between SASS and HR wind stress estimates found by Chelton et al. (1990) was apparently fortuitously consistent with previous independent conclusions by Harrison (1989) and P. Schopf (1989, personal communication) that HR wind stress estimates were too high by 17%–30%. Moreover, the differences between SASS and HR wind stress fields (see the scatterplot in Fig. 18 of Chelton et al. 1990) matched almost perfectly the 20% difference between the drag coefficients used in the two datasets.

We have repeated the comparison between SASS and HR wind stress fields over the August–September 2-month period after increasing the SASS wind stress amplitudes by 7% to account for SASS sampling errors. It is also necessary to increase the HR wind stress amplitudes by 2% because HR used a constant air density of 1.2×10^{-3} g cm^{-3} rather than the 1.223×10^{-3} value of Chelton et al. (1990). After these corrections, the HR wind stress estimates are too high by about 10%, which is smaller than the 20% difference between the two drag coefficients. Consequently, after adjusting for the difference between the HR drag coefficient and the Large and Pond (1982) drag coefficient used with the SASS data, the HR wind stress estimates are about 10% lower than SASS.

This result should not be surprising based on the analysis in section 3, which showed that the drag coefficient must be inflated by about 7% when constructing vector-averged stress fields from the irregularly spaced SASS vector wind observations. The drag coefficient should be inflated similarly for constructing climatological monthly mean wind stress fields from ship observations, which are even more irregularly distributed in space and time than the SASS data. Increasing the drag coefficient by about 10% could

apparently compensate for biases introduced by sampling errors in the ship data.

The comparison between TLO and SASS wind stress fields presented in section 4 showed that the TLO wind stress climatology is about 46% higher than SASS in extratropical northern latitudes and middle southern latitudes. From the point comparisons between ECMWF synoptic wind analyses and NDBC buoy winds, this difference is entirely consistent with an error in the TLO interpretation of 1000-mb winds as 10-m winds. Other authors have independently reached similar conclusions. Anderson et al. (1991), for example, found that the 1000-mb ECMWF winds correspond to a height of approximately 30 m, and thus must be reduced in magnitude to be compared with 10-m measurements. The systematic difference between TLO and SASS wind stress magnitudes can be eliminated by reducing the ECMWF 1000-mb wind speeds by 14% to convert the 1000-mb winds to 10-m winds prior to calculating the wind stress from the bulk aerodynamic formula. Without this 14% reduction, the ECMWF wind speeds are 16.5% too high.

If the drag coefficient were constant and wind direction steady, the 16.5% overestimate of wind speed resulting from treating the 1000-mb winds as 10-m winds would lead to a 35.7% overestimate of wind stress magnitude. However, because of the wind speed dependence of the drag coefficient [see Eq. (1)] and vector averaging of winds with unsteady speed and direction, the overestimates of the magnitudes of 2-month vector average wind stresses increase to about 45%.

It is important to emphasize that the 14% scaling factor deduced here was derived from comparisons of ECMWF winds with contemporaneous buoy winds for the 1980–1986 period. Any systematic inaccuracies in the SASS winds are therefore not an issue in the conclusion that the TLO wind stress climatology is systematically high in magnitude. Nor are land effects on the buoy winds a major concern since none of the buoys considered here were closer than 100 km to land. The major limitation of the buoy wind data is the limited geographical coverage. The primary contribution of the SASS data to this study is that they provide global coverage. The comparisons between TLO and SASS winds are entirely consistent with the scaling error in the TLO winds derived from the buoy data. This consistency is overwhelmingly strong evidence that the TLO climatology is biased high. It can also be inferred from this result that any systematic errors in the SASS winds must be small since the same conclusion about TLO errors can be deduced independently from SASS and buoy winds.

A crude method of correcting for the apparent systematic errors in the TLO climatology is to reduce each mean monthly gridded wind stress estimate by 46%. Although the scaling error probably does not deviate much from 46% throughout the year, it should be kept in mind that the analysis described in this study is restricted to the August–September time period. Owing to the wind speed and stability dependencies of the drag coefficient and the complicating effects of vector averaging in regions of low wind directional steadiness, the scaling factor may vary somewhat geographically and at other times of year. A complete analysis would require comparisons between ECMWF synoptic 1000-mb wind analyses and concurrent buoy observations for each month of the year. Using the scaling factor determined from such an analysis to convert the 1000-mb winds to 10-m winds, the complete vector-averaged monthly wind stress climatology should be recomputed as we have done here for the August–September period.

A similar scaling error in the TLO climatology is expected south of 50°S. At these high southern latitudes, however, interannual variability is large, there are no contemporaneous buoy measurements, and a systematic scaling error cannot be isolated based on comparisons with SASS data. We have argued in section 5 that a reliable estimate of mean monthly wind stress does not presently exist at high southern latitudes. Moreover, it will not be possible to construct such a field in this region of sparse conventional wind observations until a sufficiently long record of highly accurate scatterometer winds has been acquired (at least three years, and preferably five or more years). Until such time, the details of model simulations of the Antarctic Circumpolar Current must be considered tentative at best.

Acknowledgments. We thank Robert Atlas for providing the SASS vector wind data used in this investigation and Kevin Trenberth for providing the TLO mean monthly wind stress climatology, the climatological air–sea temperature difference and humidity fields and the sea surface temperature climatology used to calculate wind stress. We also thank Steve Esbensen for helpful discussions during the course of this research. The research described in this paper was supported by Contracts 957580, 957581, and 959351 from the Jet Propulsion Laboratory funded under the NSCAT Announcement of Opportunity and by NASA Grant NAGW-3062.

REFERENCES

Aagaard, K., 1969: Relationship between geostrophic and surface winds at weather ship M. *J. Geophys. Res.*, **74**, 3440–3442.

Anderson, D., A. Hollingsworth, S. Uppala, and P. Woiceshyn, 1991: A study of the use of scatterometer data. *J. Geophys. Res.*, **96**, 2619–2634.

Atlas, R., A. J. Busalacchi, M. Ghil, S. Bloom, and E. Kalnay, 1987: Global surface wind and flux fields from model assimilation of Seasat data. *J. Geophys. Res.*, **92**, 6477–6487.

Beal, R.C., 1991: *Directional Ocean Wave Spectra.* The Johns Hopkins University Press, 218 pp.

Böttger, H., 1982: Local weather element guidance from the ECMWF forecasting system in the medium range. A verification study. *Seminar/Workshop on Interpretation of Numerical Weather Predictions Products,* ECMWF, 417–441.

Chelton, D. B., and F. J. Wentz, 1986: Further development of an improved altimeter wind speed algorithm. *J. Geophys. Res.*, **91**, 14 250–14 260.

——, M. H. Freilich, and J. R. Johnson, 1989: Evaluation of unambiguous vector winds from the Seasat scatterometer. *J. Atmos. Oceanic Technol.*, **6**, 1024–1039.

——, A. M. Mestas-Nuñez, and M. H. Freilich, 1990: Global wind stress and Sverdrup circulation from the Seasat scatterometer. *J. Phys. Oceanogr.*, **20**, 1175–1205.

Clarke, R. H., and G. D. Hess, 1975: On the relation between surface wind and pressure gradient, especially in lower latitudes. *Bound.-Layer Meteor.*, **9**, 325–339.

Davison, J., and D. E. Harrison, 1990: Comparison of Seasat scatterometer winds with tropical Pacific observations. *J. Geophys. Res.*, **95**, 3403–3410.

Dittmer, K., 1977: The hydrodynamic roughness of the sea surface at low wind speeds. *Meteor. Forsch.-Ergebnisse, Reihe B,* **12**, 10–15.

Findlater, J., T. N. S. Harrower, G. A. Howkins, and H. L. Wright, 1966: Surface and 900 mb wind relationships. Scientific Paper No. 23, UKMO, 41 pp. [Available from the UK Meteorological Office, London Road, Bracknell, Berkshire, RG12 2SZ, UK.]

Freilich, M. H., and R. S. Dunbar, 1993: Derivation of satellite wind model functions using operational surface wind analyses: An altimeter example. *J. Geophys. Res.*, **98**, 14 633–14 649.

Godfrey, J. S., 1989: A Sverdrup model of the depth-integrated flow for the World Ocean allowing for island circulations. *Geophys. Astrophys. Fluid Dyn.*, **45**, 89–112.

Harrison, D. E., 1989: On climatological monthly mean wind stress and wind stress curl fields over the World Ocean. *J. Climate*, **2**, 57–70.

Hasse, L., and V. Wagner, 1971: On the relationship between geostrophic and surface wind at sea. *Mon. Wea. Rev.*, **99**, 255–260.

Hellerman, S., and M. Rosenstein, 1983: Normal monthly wind stress over the World Ocean with error estimates. *J. Phys. Oceanogr.*, **13**, 1093–1104.

Janssen, P. A. E. M., P. Lionello, M. Reistad, and A. Hollingsworth, 1989: Hindcasts and data assimilation studies with the WAM model during the Seasat period. *J. Geophys. Res.*, **94**, 973–993.

Kelly, K. A., and M. J. Caruso, 1990: A modified objective mapping technique for scatterometer wind data. *J. Geophys. Res.*, **95**, 13 483–13 496.

Lalbeharry, R., M. L. Khandekar, and S. Peteherych, 1990: Wind specification based on Seasat A satellite scatterometer and conventional winds for driving an ocean wave model. *J. Geophys. Res.*, **95**, 761–773.

Lambert, S. J., 1988: A comparison of operational global analyses from the European Centre for Medium-Range Weather Forecasts (ECMWF) and the National Meteorological Center (NMC). *Tellus*, **40A**, 272–284.

Large, W. G., and S. Pond, 1982: Sensible and latent heat flux measurements over the ocean. *J. Phys. Oceanogr.*, **12**, 464–482.

Legler, D. M., and J. J. O'Brien, 1985: Development and testing of a simple assimilation technique to derive average wind fields from simulated scatterometer data. *Mon. Wea. Rev.*, **113**, 1791–1800.

Lionello, P., H. Günther, and P. A. E. M. Janssen, 1992: Assimilation of altimeter data in a global third-generation wave model. *J. Geophys. Res.*, **97**, 14 453–14 474.

Liu, W. T., K. B. Katsaros, and J. A. Businger, 1979: Bulk parameterization of air–sea exchange in heat and water vapor including the molecular constraints at the interface. *J. Atmos. Sci.*, **36**, 1722–1735.

Meindl, E. A., and G. D. Hamilton, 1992: Programs of the National Data Buoy Center. *Bull. Amer. Meteor. Soc.*, **73**, 985–993.

Mestas-Nuñez, A. M., D. B. Chelton, and R. A. deSzoeke, 1992: Evidence of time-dependent Sverdrup circulation in the South Pacific from the Seasat scatterometer and altimeter. *J. Phys. Oceanogr.*, **22**, 934–943.

Reynolds, R. W., K. Arpe, C. Gordon, S. P. Hayes, A. Leetmaa, and M. J. McPhaden, 1989: A comparison of tropical Pacific surface winds analyses. *J. Climate*, **2**, 105–111.

Schacher, G. E., K. L. Davidson, T. E. Houlihan, and C. W. Fairall, 1981: Measurements of the rate of dissipation of turbulent kinetic energy, ϵ, over the ocean. *Bound.-Layer Meteor.*, **20**, 321–330.

Schaefer, J. T., and C. A. Doswell III, 1979: On the interpolation of a vector field. *Mon. Wea. Rev.*, **107**, 458–476.

Shea, D. J., K. E. Trenberth, and R. W. Reynolds, 1990: A global monthly sea surface temperature climatology. National Center for Atmos. Res. Tech. Note, NCAR/TN-345 +STR, 167 pp.

Trenberth, K. E., 1984: Interannual variability of the Southern Hemisphere circulation: Representativeness of the year of the Global Weather Experiment. *Mon. Wea. Rev.*, **112**, 108–123.

——, and H. van Loon, 1981: Comment on "Impact of FGGE buoy data on Southern Hemisphere analyses." *Bull. Amer. Meteor. Soc.*, **62**, 1486–1489.

——, and J. R. Christy, 1985: Global fluctuations in the distribution of atmospheric mass. *J. Geophys. Res.*, **90**, 8042–8052.

——, J. G. Olson, and W. G. Large, 1989: A global ocean wind stress climatology based on ECMWF analyses. National Center for Atmos. Res. Tech. Note, NCAR/TN-338 +STR, 93 pp.

——, W. G. Large, and J. G. Olson, 1990: The mean annual cycle in global ocean wind stress. *J. Phys. Oceanogr.*, **20**, 1742–1760.

Wentz, F. J., L. A. Mattox, and S. Peteherych, 1986: New algorithms for microwave measurements of ocean winds with application to Seasat and SSM/I. *J. Geophys. Res.*, **21**, 2289–2307.

Willebrand, J., 1978: Temporal and spatial scales of the wind field over the North Pacific and North Atlantic. *J. Phys. Oceanogr.*, **8**, 1080–1094.